Supplementary Information for

Topological control of metal–organic frameworks towards highly sensitive and selective detection of chromate and dichromate

Zi-Jian Li,[a] Yu Ju,[a,c] Xiao-Ling Wu,[a] Xiaoyun Li, [a] Jie Qiu,[b] Yongxin Li[d], Zhi-Hui Zhang,[c] Ming-Yang He,[c] Linjuan Zhang,[a] Jian-Qiang Wang,[a] and Jian Lin[*,b]

[a]Key Laboratory of Interfacial Physics and Technology, Shanghai Institute of Applied Physics, Chinese Academy of Sciences, Shanghai 201800, China.

[b]School of Nuclear Science and Technology, Xi'an Jiaotong University, No.28, West Xianning Road, Xi'an, 710049, P. R. China. E-mail: jianlin@xjtu.edu.cn

[c]Jiangsu Key Laboratory of Advanced Catalytic Materials and Technology, Changzhou University, Changzhou 213164, China

[d]Division of Chemistry and Biological Chemistry, School of Physical and Mathematical Sciences, Nanyang Technological University, 637371, Singapore

*Co-corresponding authors

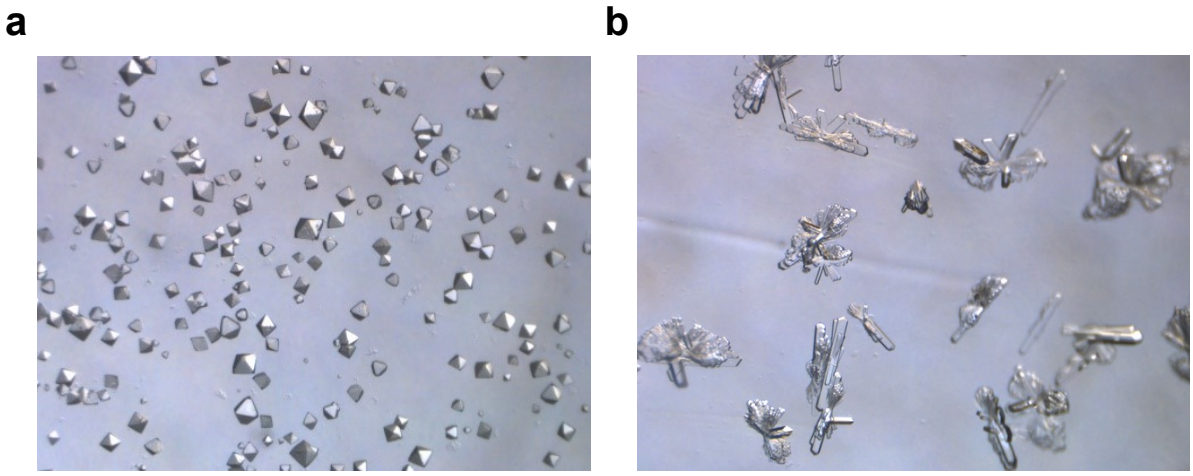

Fig. S1 Crystal images of (a) **Th-BCTPE-1** and (b) **Th-BCTPE-2**.

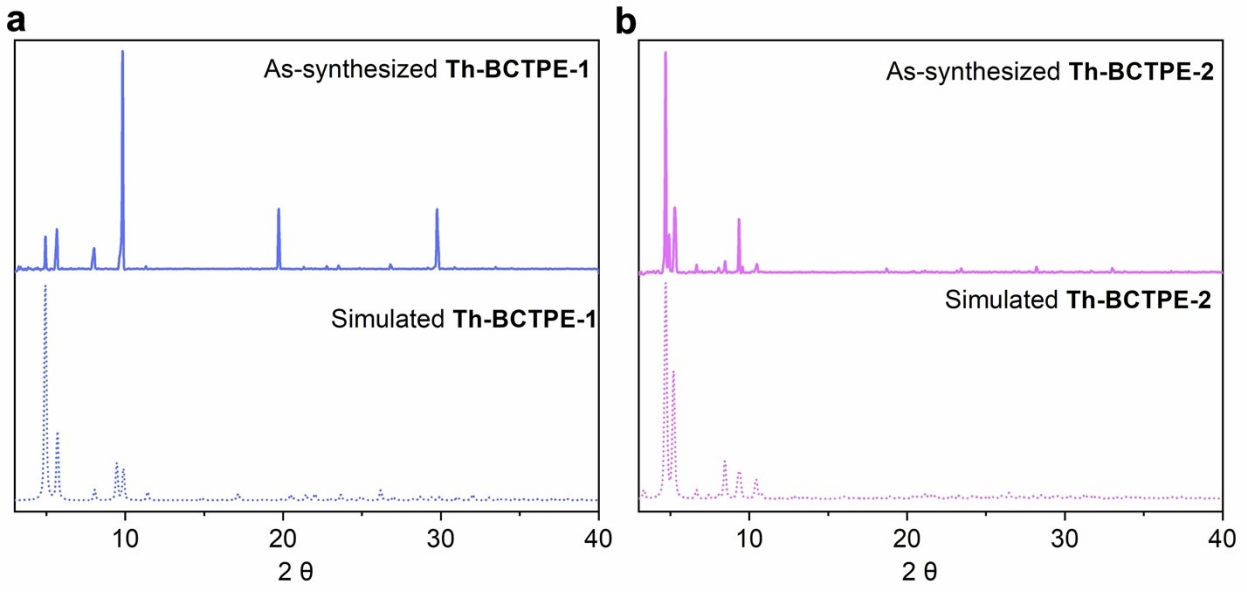

Fig. S2 Powder X-ray diffraction patterns of as-synthesized and simulated (b) **Th-BCTPE-1** and (b) **Th-BCTPE-2**.

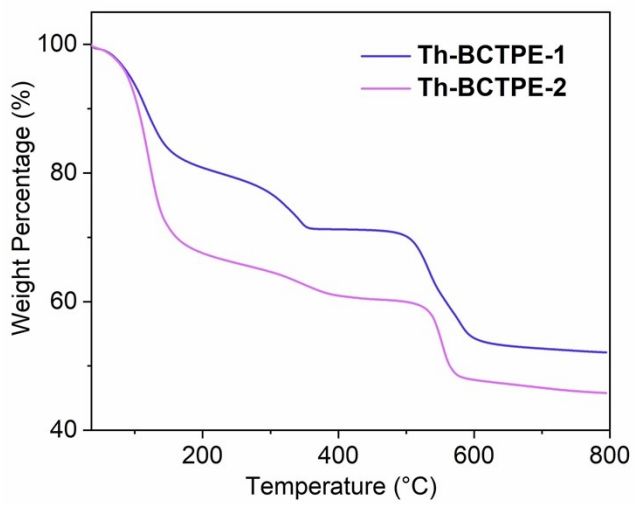

Fig. S3 Thermogravimetric analysis (TGA) curves of **Th-BCTPE-1** and **Th-BCTPE-2**.

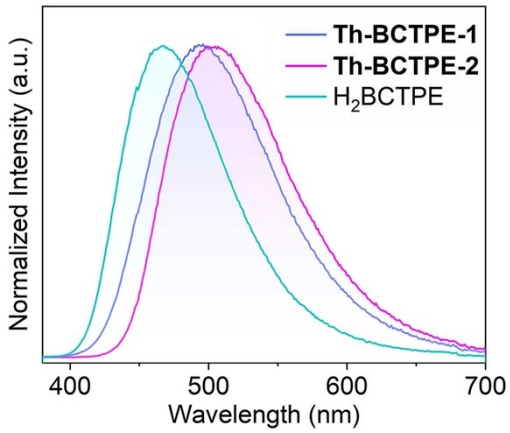

Fig. S4 Photoluminescence spectra of **Th-BCTPE-1**, **Th-BCTPE-2**, and H_2BCTPE under 365 UV excitation.

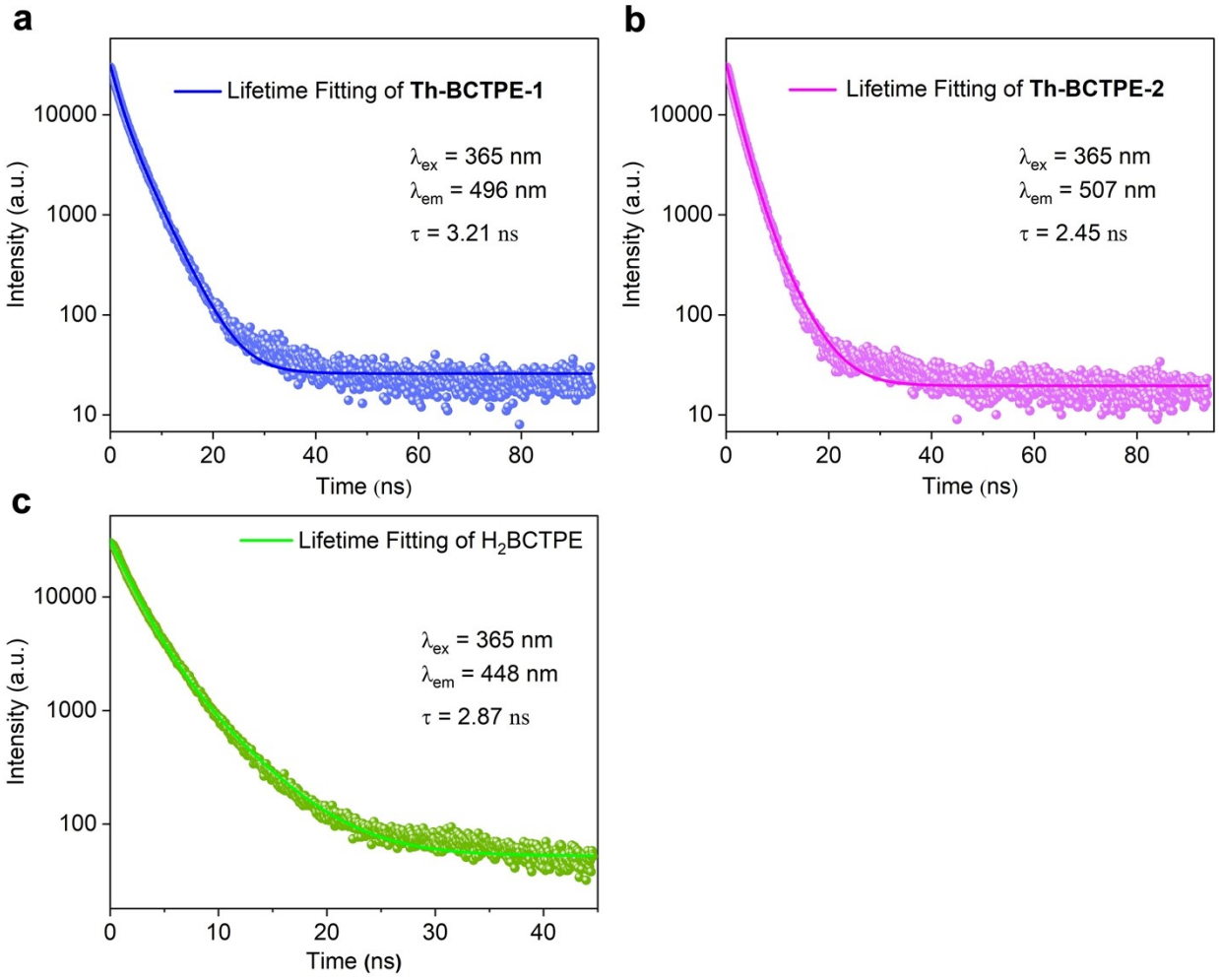

Fig. S5 Photoluminescence lifetimes of **Th-BCTPE-1**, **Th-BCTPE-2**, and H_2BCTPE.

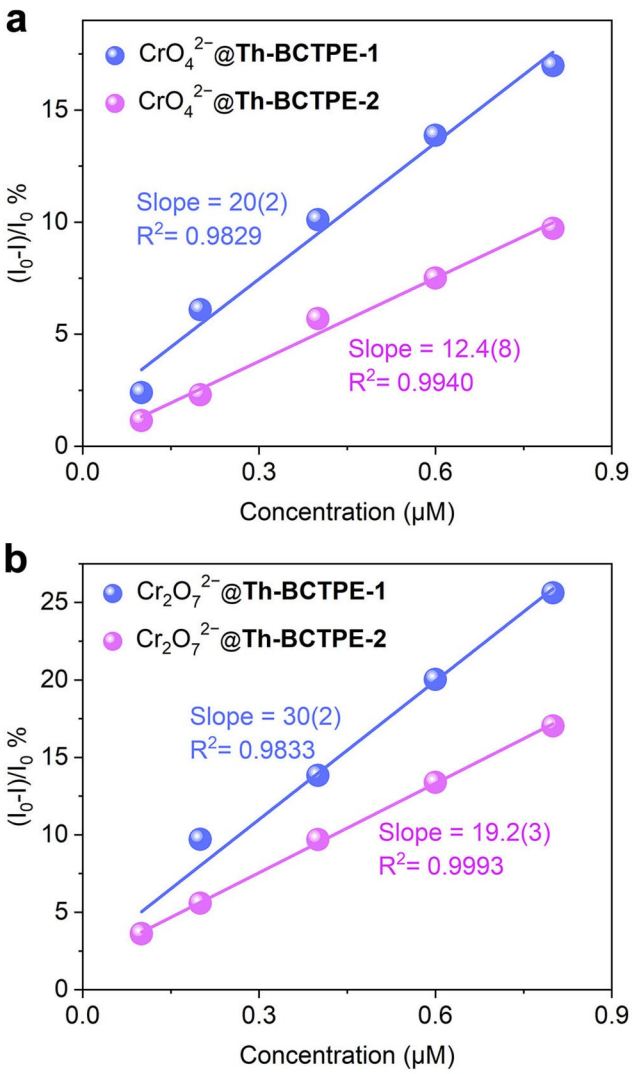

Fig. S6 The quenching rates of **Th-BCTPE-1 and Th-BCTPE-2** as a function of (a) CrO_4^{2-} and (b) $Cr_2O_7^{2-}$ concentration (0.1 – 0.9 μM).

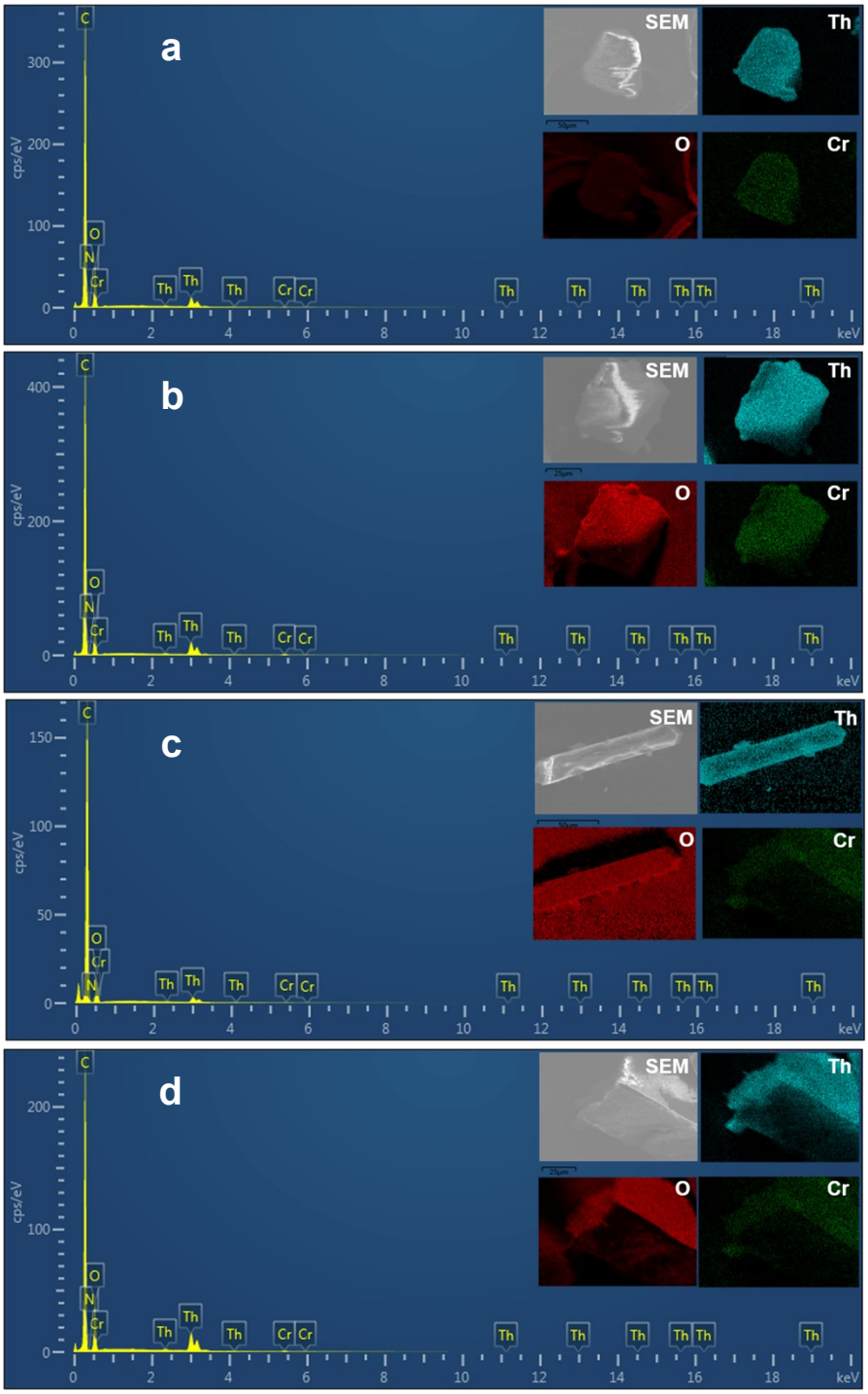

Fig. S7 (a) SEM–EDS mapping and spectrum of CrO_4^{2-} soaked **Th-BCTPE-1**. (b) SEM–EDS mapping and spectrum of $Cr_2O_7^{2-}$ soaked **Th-BCTPE-1**. (c) SEM–EDS mapping and spectrum of CrO_4^{2-} soaked **Th-BCTPE-2**. (d) SEM–EDS mapping and spectrum of $Cr_2O_7^{2-}$ soaked **Th-BCTPE-2**.

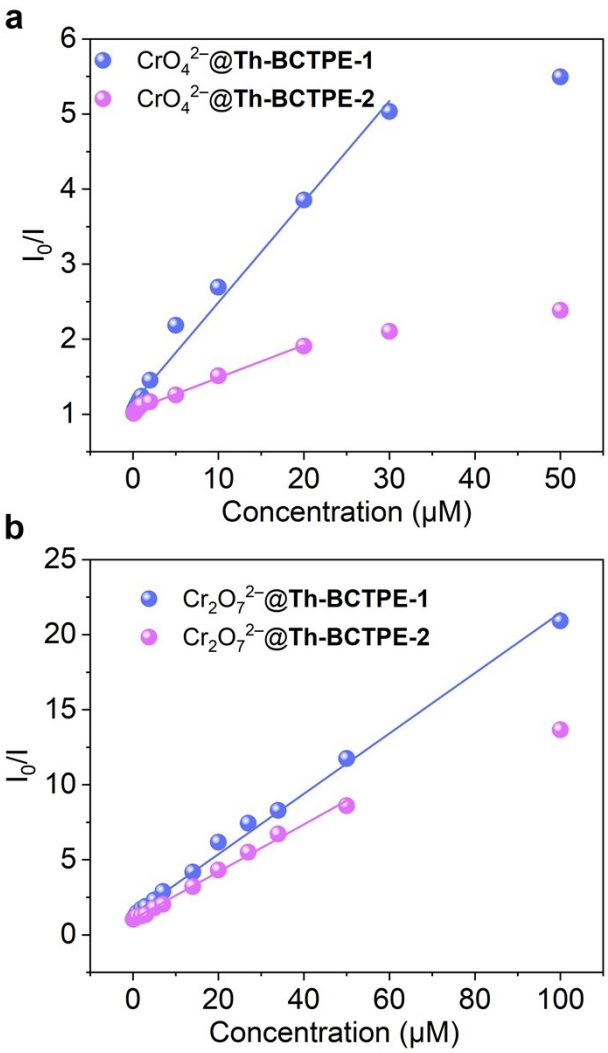

Fig. S8 The correlations of I_0/I as a function of (a) CrO_4^{2-} and (b) $Cr_2O_7^{2-}$ concentrations at high concentraiton region.

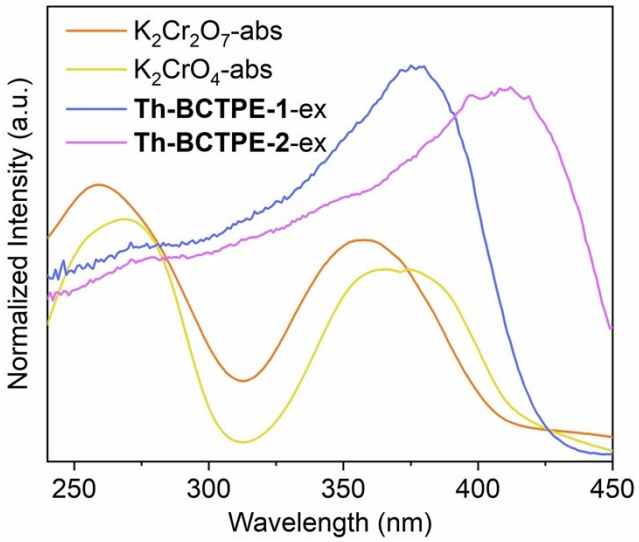

Fig. S9 The absorption spectra of K_2CrO_4 / $K_2Cr_2O_7$ solution and the excitation spectra of **Th-BCTPE-1** and **Th-BCTPE-2**.

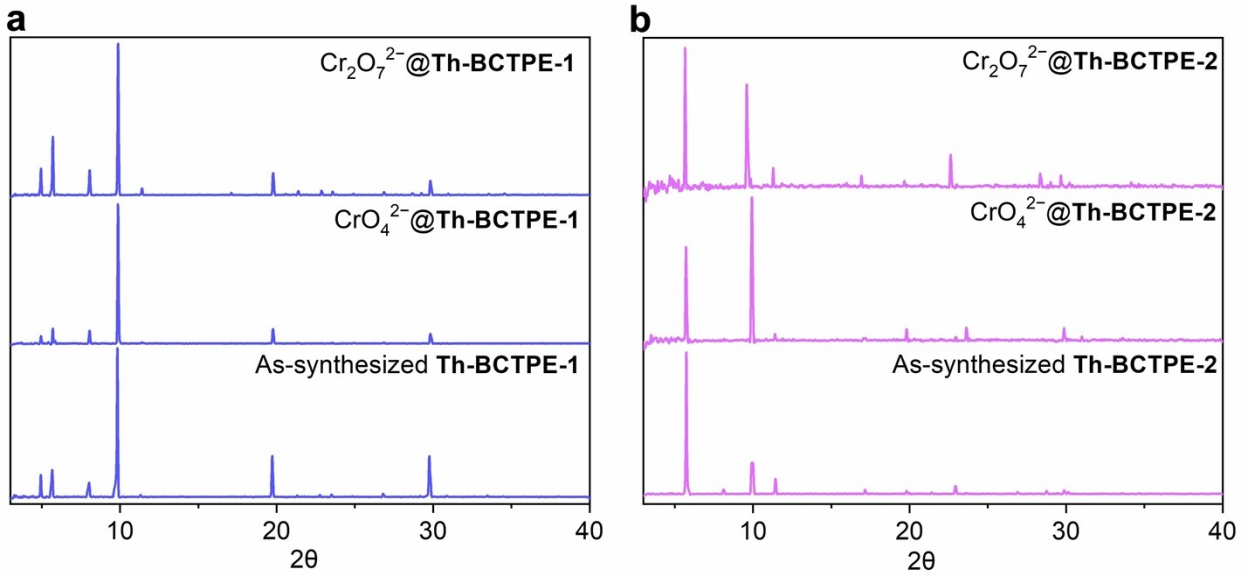

Fig. S10 Powder X-ray diffraction patterns of as-synthesized, CrO_4^{2-} soaked, and $Cr_2O_7^{2-}$ soaked (a) **Th-BCTPE-1** and (b) **Th-BCTPE-2**.

Table S1 Crystallographic data for **Th-BCTPE-1** and **Th-BCTPE-2**.

Code	**Th-BCTPE-1**	**Th-BCTPE-2**
CCDC No.	2213561	2213562
formula	$C_{336}H_{216}O_{76}Th_{12}$	$C_{141}H_{91}O_{36}Th_{6}$
formula weight	8253.55	3753.37
habit	octahedron	needle
space Group	*Fm*-3*m*	$P4_2/mmc$
a (Å)	31.000(5)	26.574(3)
b (Å)	31.000(5)	26.574(3)
c (Å)	31.000(5)	22.081(2)
α	90	90
β	90	90
γ	90	90
V (Å^3)	29790(13)	15593(3)
Z	2	2
T (K)	120	120
λ (Å)	0.71073	0.71073
Max. 2θ (°)	62.958	63.11
ρ_{calcd} (g cm^{-3})	0.920	0.799
μ (mm^{-1})	3.024	2.884
GoF on F^2	1.081	1.025
R_1, wR_2 [I > 2σ(I)]	0.0944, 0.2532	0.0977, 0.2678
R_1, wR_2 (all data)	0.1373, 0.2845	0,1477, 0.2971
$(\Delta\rho)_{max}$, $(\Delta\rho)_{min}$/e (Å^{-3})	1.59/-2.10	4.79, -5.02

Table S2 Fitting results of the Cr(VI) sorption isotherms of **Th-BCTPE-1** and **Th-BCTPE-2** according to the Langmuir and Freundlich models.

Sample	Langmuir model			Freundlich model		
	Q_m(mol/mol)	K_L (mM^{-1})	R^2	k_F (mol/mol)	n	R^2
CrO_4^{2-}@**Th-BCTPE-1**	1.5830	276.07	0.9977	1.7055	17.43	0.8781
$Cr_2O_7^{2-}$@**Th-BCTPE-1**	1.2199	43.90	0.9655	1.3564	5.53	0.6778
CrO_4^{2-}@**Th-BCTPE-2**	1.0493	60.05	0.9907	1.1671	7.05	0.8500
$Cr_2O_7^{2-}$@**Th-BCTPE-2**	0.9267	81.77	0.9635	1.1495	5.18	0.8178

Table S3 The K_{SV} and LODs of selected MOF based sensors for chromate or dichromate.

MOFs	analyte	K_{SV} (M^{-1})	LOD (M)
$[Zn_2(tpeb)_2(2,3\text{-}ndc)_2]\cdot H_2O$ [1]	CrO_4^{2-}	N/A	7.23×10^{-9}
	$Cr_2O_7^{2-}$	N/A	8.58×10^{-9}
Cd(TPA)(BIYB) [1]	$Cr_2O_7^{2-}$	1.4×10^{7}	2.4×10^{-7}
$Zn_2(H_2BCA)_2(o\text{-}bimb)_2(H_2O)_2$ [1]	CrO_4^{2-}		1.3×10^{-7}
	$Cr_2O_7^{2-}$	6.6×10^{4}	7.0×10^{-8}
$[Zn(H_2BCA)(m\text{-}bib)]\cdot H_2O$ [1]	CrO_4^{2-}		1.4×10^{-7}
	$Cr_2O_7^{2-}$	5.3×10^{4}	7.0×10^{-8}
$[Zn_2(BDC)_{1.5}(L_{16})(DMF)]\cdot 1.5DMF$ [1]	CrO_4^{2-}	6.1×10^{5}	3.0×10^{-8}
	$Cr_2O_7^{2-}$	1.0×10^{6}	2.0×10^{-8}
Hf-MOF-1 [2]	$Cr_2O_7^{2-}$	7.1×10^{4}	1.38×10^{-7}
Hf-MOF-2 [2]	$Cr_2O_7^{2-}$	4.6×10^{4}	1.38×10^{-7}
Hf-MOF-3 [2]	$Cr_2O_7^{2-}$	4.5×10^{5}	1.3×10^{-8}
$[Zn_2(tpeb)(bpdc)_2]$ [3]	CrO_4^{2-}	1.085×10^{4}	1.07×10^{-6}
	$Cr_2O_7^{2-}$	1.122×10^{4}	1.04×10^{-6}
$[Zr_6O_4(OH)_8(H_2O)_4(sbtc)_2]$ (BUT-28) [4]	$Cr_2O_7^{2-}$	1.122×10^{5}	1.7×10^{-6}
$Zr_6(OH)_{16}(TBAPy)_2$ (NU-1000) [5]	$Cr_2O_7^{2-}$	1.34×10^{4}	1.8×10^{-6}
$Zr_6O_4(OH)_{7(}H_2O)_3(BTBA)_3$ (BUT-39) [6]	$Cr_2O_7^{2-}$	1.57×10^{4}	1.5×10^{-6}
Th-BCTPE-1	CrO_4^{2-}	$2.4(1)\times10^{5}$	9.0×10^{-9}
	$Cr_2O_7^{2-}$	$4.63(3)\times10^{5}$	1.59×10^{-7}
Th-BCTPE-2	CrO_4^{2-}	$1.30(7)\times10^{5}$	4.6×10^{-9}
	$Cr_2O_7^{2}$	$2.222(9)\times10^{5}$	9.4×10^{-8}

Table S4 Calculations of LOD of **Th-BCTPE-1** and **Th-BCTPE-2**.

Sample	k_{SV} (M^{-1})	σ	LOD = 3σ/slope (nM)
CrO_4^{2-}@**Th-BCTPE-1**	2.4×10^5	0.00071	9.0
$Cr_2O_7^{2-}$@**Th-BCTPE-1**	4.6×10^5	0.00071	4.6
CrO_4^{2-}@**Th-BCTPE-2**	1.30×10^5	0.0069	159
$Cr_2O_7^{2-}$@**Th-BCTPE-2**	2.222×10^5	0.0069	94

Supplementary References

1. B. Parmar, K. K. Bisht, Y. Rachuri and E. Suresh, *Inorg. Chem. Front.*, 2020, **7**, 1082.
2. K. Wu, J. Zheng, Y.-L. Huang, D. Luo, Y. Y. Li, W. Lu and D. Li, *J. Mater. Chem. C*, 2020, **8**, 16974.
3. B. B. Rath and J. J. Vittal, *Inorg. Chem.*, 2020, **59**, 8818.
4. M.-M. Xu, X.-J. Kong, T. He, X.-Q. Wu, L.-H. Xie and J.-R. Li, *Inorg. Chem.*, 2018, **57**, 14260.
5. Z.-J. Lin, H.-Q. Zheng, H.-Y. Zheng, L.-P. Lin, Q. Xin and R. Cao, *Inorg. Chem.*, 2017, **56**, 14178.
6. T. He, Y.-Z. Zhang, X.-J. Kong, J. Yu, X.-L. Lv, Y. Wu, Z.-J. Guo and J.-R. Li, *ACS Appl. Mater. Interfaces*, 2018, **10**, 16650.